A search for human influences on the thermal structure of the atmosphere

B. D. Santer*, K. E. Taylor*†, T. M. L. Wigley‡, T. C. Johns§, P. D. Jones‖, D. J. Karoly¶, J. F. B. Mitchell§, A. H. Oort#, J. E. Penner†, V. Ramaswamy#, M. D. Schwarzkopf#, R. J. Stouffer# & S. Tett§

* Program for Climate Model Diagnosis and Intercomparison, † Atmospheric Science Division, Lawrence Livermore National Laboratory, Livermore, California 94550, USA
‡ National Center for Atmospheric Research, Boulder, Colorado 80307-3000, USA
§ Hadley Centre for Climate Prediction and Research, Meteorological Office, Bracknell RG12 2SY, UK
‖ Climatic Research Unit, University of East Anglia, Norwich NR4 7TJ, UK
¶ Cooperative Research Centre for Southern Hemisphere Meteorology, Monash University, Clayton VIC 3168, Australia
# NOAA/Geophysical Fluid Dynamics Laboratory, PO Box 308, Princeton University, Princeton, New Jersey 08542, USA

The observed spatial patterns of temperature change in the free atmosphere from 1963 to 1987 are similar to those predicted by state-of-the-art climate models incorporating various combinations of changes in carbon dioxide, anthropogenic sulphate aerosol and stratospheric ozone concentrations. The degree of pattern similarity between models and observations increases through this period. It is likely that this trend is partially due to human activities, although many uncertainties remain, particularly relating to estimates of natural variability.

CHANGES in the vertical structure of atmospheric temperature have been proposed as a possible 'fingerprint' of greenhouse-gas-induced climate change[1–4]. Until recently, most of the information about such a fingerprint resulted from experiments in which an atmospheric general circulation model (AGCM) coupled to a mixed-layer ocean was forced by a doubling of atmospheric CO_2 levels.[5,6] For annually averaged changes, these experiments show a hemispherically symmetrical pattern of stratospheric cooling and tropospheric warming, with a warming maximum in the tropical upper troposphere (Fig. 1*a*). One recent study[7] compared such model-predicted signals with observed radiosonde measurements[8] and concluded that this fingerprint was increasingly evident in observed data. The degree of time-increasing similarity was judged to be statistically significant—that is, unlikely to be due to natural climate variability alone.

The work reported here differs from this earlier work in four respects. First, we examine the relative detectability of vertical temperature-change signals due to individual and combined changes in atmospheric CO_2 and anthropogenic sulphate aerosols[9,10]. Previous detection work involving temperature changes in the free atmosphere has used signals due to increases in CO_2 only. We consider signals due to combined CO_2 and aerosol forcing because recent studies of near-surface temperature changes show that a combined signal may be easier to identify in the observations than a signal due to changes in CO_2 alone[10,11].

Second, we use signal data from two different models in order to explore the sensitivity of our results to model-dependent uncertainties in the definition of an anthropogenic signal. These uncertainties arise from model differences in physics, resolution, representation of aerosol effects, and modelling strategy.

Third, we consider how a combined CO_2 + aerosol vertical temperature-change signal might be modified by observed changes in stratospheric ozone. The observed reduction in stratospheric ozone over the past two decades is attributable largely to the industrial production of halocarbons[12]. One recent study in which an AGCM was forced by changes in both CO_2 and stratospheric ozone showed that the inclusion of ozone effects improves model agreement with the radiosonde temperature data, particularly in the upper troposphere[13,14]. As results are not yet available from experiments with combined changes in CO_2, anthropogenic sulphate aerosols and stratospheric ozone, we perform a simple sensitivity study of possible ozone effects by linearly combining results from CO_2 + aerosol[9] and ozone-only[15] model studies.

Fourth, we use information from three long control runs performed with coupled atmosphere–ocean GCMs (CGCMs) to assess the significance of trends in model-versus-observed pattern similarity. Such integrations provide estimates of internally generated natural climate variability on a range of space and timescales. Comparable information on the multi-decadal natural climate variability crucial to the detection problem is impossible to obtain from the short (<40-year) radiosonde temperature record.

Model signals and observational data

We use model data from experiments with fixed levels of anthropogenic pollutants ('equilibrium experiments') and from integrations in which the atmospheric concentrations of greenhouse gases and aerosols increase over time ('transient experiments'). The equilibrium CO_2-only and CO_2 + aerosol vertical temperature-change signals were taken from experiments performed by Taylor and Penner[9] (henceforth TP) with a tropospheric chemistry model[16,17] coupled to an AGCM with a simple mixed-layer ocean[18]. The chemistry–climate model considers only the direct radiative effects of sulphate aerosols (reflection of incident solar radiation)[19]. In addition to a control run with nominal pre-industrial levels of CO_2 (270 parts per million by volume, p.p.m.v.) and no anthropogenic sulphur emissions, three perturbation experiments were performed: a sulphate-only experiment (S-TP) with near-present-day anthropogenic sulphur emissions, a CO_2-only experiment (C-TP) with near-present-day CO_2 levels (345 p.p.m.v.), and an experiment with combined present-day CO_2 levels and anthropogenic sulphur emissions (SC-TP)[9]. The differences between the perturbation experiments and the control represent equilibrium changes from pre-industrial to present-day conditions.

We also consider vertical temperature-change signals from two

recent transient experiments performed with the Hadley Centre (henceforth HC) CGCM[10,20]. The model has full ocean dynamics, and was forced over 1860 to 1990 with historical increases in greenhouse gases only (C-HC) and with increases in both greenhouse gases and anthropogenic SO_2 emissions (SC-HC). After 1990 the concentration of SO_2 evolved according to IPCC Scenario IS92a[21] while the concentration of equivalent CO_2 increased at 1% per year. Direct scattering effects of aerosols are represented by changes in the surface albedo[22].

To study how a reduction in stratospheric O_3 might modify the SC signal pattern, we use data from an experiment performed with the Geophysical Fluid Dynamics Laboratory (GFDL) 'SKYHI' atmospheric GCM[15]. The model was forced with observed monthly-mean zonal average changes in stratospheric ozone over the period 1979–90, and was run with fixed cloud distributions in the troposphere and sea-surface temperature prescribed according to climatology. An idealized vertical structure of ozone losses was imposed, with constant percentage reductions in an atmospheric region extending from the tropopause to roughly 7 km above[15].

The radiosonde temperature analyses were available as anomalies for December–January–February (DJF), June–July–August (JJA) and annually averaged data relative to a reference period of 1963–73, and spanned the period 1963–87[8]. The data are in the form of zonal averages for seven atmospheric levels (850, 700, 500, 300, 200, 100 and 50 hPa). The principal data uncertainties have been described previously[7,8,23].

Comparisons between the radiosonde data and satellite-derived estimates of vertical temperature changes indicate that the two data sets are in good agreement over the period of overlap, at least in terms of the global[24] and hemispheric[8] means. For the present study we compared the radiosonde data with a reanalysis of operationally produced climate data[25]. The seasonal patterns of (zonally averaged) linear trends as a function of latitude and height were in close agreement for the period of overlap between the two data sets (1979–87), despite differences in the spatial coverage of the radiosonde data (primarily land only) and the reanalysis (land + ocean).

Note that the amplitudes of the observed changes and model signals are not directly comparable, as they represent responses to radiative forcing changes over different periods. If the radiative forcing histories and lags between forcing and response were known exactly for O_3, CO_2 and sulphate aerosols, it would be possible to make a more meaningful comparison of the amplitudes of observed and modelled vertical temperature changes by scaling according to differences in overall response. Large forcing uncertainties, particularly for sulphate aerosol effects, make such scaling exercises very difficult. We circumvent some of these difficulties by using a comparison statistic that focuses on patterns rather than amplitudes of temperature change. The issue of amplitude differences is important in the linear superposition of O_3 and SC signals, and we return to it later.

Patterns of vertical temperature change

Modelled and observed patterns of annual-mean zonal-mean temperature change as a function of latitude and height are shown in Fig. 1. The pattern of stratospheric cooling and tropospheric warming in C-TP (Fig. 1*a*) is in accord with previous modelling work[5–7] and represents the direct radiative signature of the change in CO_2. Maximum warming occurs in the tropical upper troposphere, and temperature changes are hemispherically symmetric. In contrast, both the S-TP (Fig. 1*b*) and SC-TP (Fig. 1*c*) signals show a hemispherically asymmetric response, with (respectively) increased cooling and reduced warming in the Northern Hemisphere, where anthropogenic sulphate aerosol forcing is largest[9,22]. The SC-TP integration (like C-TP) also shows the dipole structure of stratospheric cooling/tropospheric warming characteristic of CO_2 changes, whereas there is minimal stratospheric response in S-TP.

The C-HC and SC-HC transient results (Fig. 1*d*, *e*) have features which are qualitatively similar to the equilibrium response patterns from the corresponding TP experiments (Fig. 1*a*, *c*). Both types of experiment yield stratospheric cooling and tropospheric warming (C and SC) and reduced warming in the Northern Hemisphere (SC only). We return to this point later, because it is relevant to the issue of the usefulness of equilibrium signals in climate-change detection studies.

Vertical temperature changes due to stratospheric O_3 reduction (Fig. 1*f*) are characterized by stratospheric cooling, with maximum cooling at high latitudes in both hemispheres. Owing to dynamical effects, cooling occurs throughout the lower stratosphere, even at low latitudes where the imposed ozone changes are negligible[15,26]. The response is not hemispherically symmetric: stratospheric cooling that is statistically significant[15] occurs over a wider latitude range in the Northern Hemisphere than in the Southern Hemisphere. This is primarily due to a hemispheric asymmetry in the observed ozone changes. Some of the model–observed temperature differences in Fig. 1*f* and *j*, such as the warming above about 70 hPa poleward of 45° S, are probably related to the idealized altitudinal profile of ozone loss[26]. Other differences are due to the different time periods considered in the model experiment and in the observations.

To examine the possible effects of stratospheric O_3 depletion we perform two sensitivity studies. COMB1 is the unweighted sum of the SC-TP and O_3 signals (Fig. 1*g*). COMB2 (Fig. 1*h*) explores uncertainties in the relative amplitudes of the SC-TP and O_3 signal components by halving the amplitude of the SC-TP signal. A third sensitivity study (COMB3; Fig. 1*i*), considers the effect of uncertainties in the magnitude of the aerosol forcing (and response) by halving the amplitude of the S-TP signal relative to the C-TP signal.

For any of these sensitivity experiments to be a realistic estimate of the response to combined $CO_2 + SO_4 + O_3$ forcing requires the relative weights of the individual forcings to be realistic and the climate system to respond quasi-linearly to perturbations. We have tested this linear superposition assumption and found it to be valid for combining the C-TP and S-TP signals[27]. The assumption cannot be tested for the HC experiments (owing to the lack of a transient experiment with forcing by aerosol effects alone) or for O_3 effects (because suitable model studies with individual and combined forcing by $CO_2 + SO_4 + O_3$ were not available). A linear combination of O_3 and SC effects is probably reasonable above the tropopause[28].

Incorporating stratospheric ozone effects (COMB1, COMB2) intensifies stratospheric cooling and reduces the height of the

FIG. 1 Modelled and observed zonal-mean annually averaged changes (°C) in the thermal structure of the atmosphere. The equilibrium experiments by Taylor and Penner (TP)[9] simulate temperature changes for nominal 'present-day' levels of atmospheric CO_2 only (C-TP; *a*), anthropogenic sulphate aerosols only (S-TP; *b*), and combined forcing by CO_2 + sulphate aerosols (SC-TP; *c*) relative to a control run with pre-industrial levels of CO_2 and no anthropogenic sulphur emissions. All TP integrations were at least 30 years in duration, and temperature-change signals were computed using averages over the last 20 years of the control run and each perturbation experiment. Patterns of the response to time-varying increases in greenhouse gases only (C-HC; *d*) and in greenhouse gases and aerosols (SC-HC; *e*) were taken from simulations performed with the Hadley Centre CGCM[10,20]. Temperature-change signals are the decadal averages of C-HC and SC-HC for the modelled '1990s' expressed relative to the respective C-HC and SC-HC averages over 1880–1920. The possible effects of stratospheric ozone reduction over the period 1979–90 (*f*) are from a recent equilibrium experiment by Ramaswamy *et al.*[15] The sensitivity studies COMB1 (SC-TP + O_3; *g*) and COMB2 ($\frac{1}{2}$SC-TP + O_3; *h*) consider the possible effects of stratospheric O_3 depletion on the SC-TP signal. COMB3 ($\frac{1}{2}$S-TP + C-TP; *i*) illustrates the sensitivity of model-observed pattern similarities to a possible overestimate of direct aerosol effects in TP. Observed changes (*j*) are radiosonde-based temperature measurements from the data set by Oort[8], and are expressed as total least-squares linear trends (°C) over the 25-year period extending from May 1963 to April 1988.

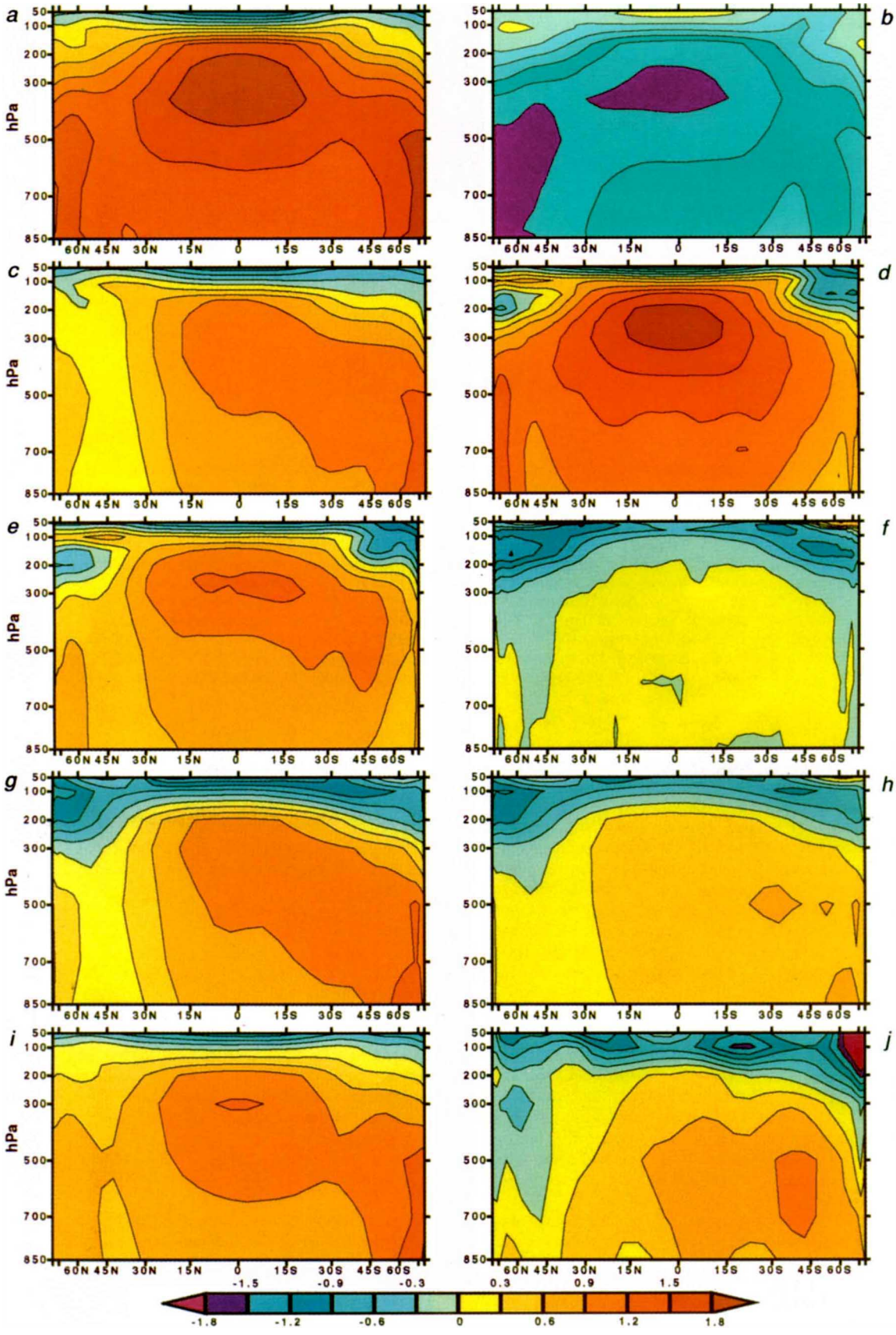
a
b
c
d
e
f
g
h
i
j
hPa
50
100
200
300
500
700
850
60N 45N 30N 15N 0 15S 30S 45S 60S
-1.5 -0.9 -0.3 0.3 0.9 1.5
-1.8 -1.2 -0.6 0 0.6 1.2 1.8

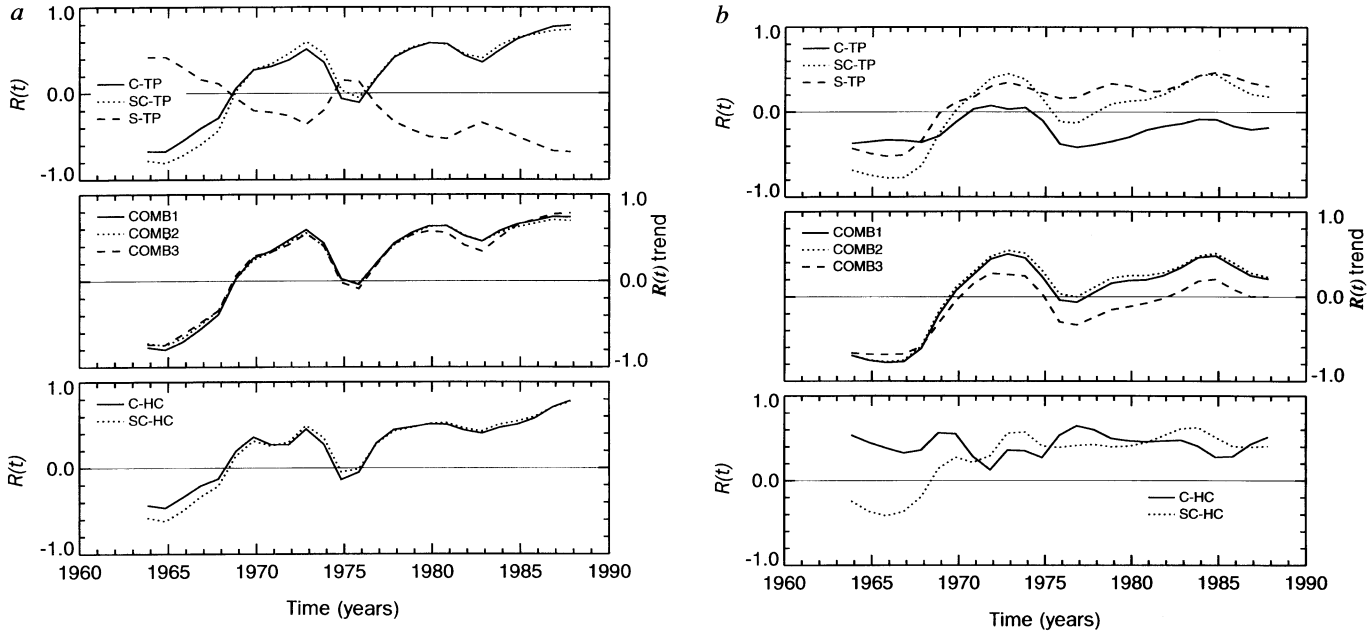

FIG. 2 Time series of centred pattern correlations, $R(t)$, between model-predicted and observed changes in zonal-mean latitude–height profiles of atmospheric temperature. For sources of model and observed data, refer to Fig. 1. Observed changes are expressed as a sequence of anomaly patterns spanning the period 1963–87, and were smoothed with a 5-term binomial filter to suppress variability on timescales shorter than a decade (for example, associated with ENSO events and the quasi-biennial oscillation)[11]. For each model experiment, one pattern characterizes the response to the imposed anthropogenic forcing (see Fig. 1). This fixed pattern is correlated with the observed time-varying spatial patterns. Results are for temperature-change patterns defined over the full vertical extent of the radiosonde data (50–850 hPa; *a*) and over the mid- to lower-troposphere only (500–850 hPa; *b*). The premise underlying the use of a centred correlation for attribution is that different 'causes' (forcing mechanisms) have different response patterns. If one can demonstrate time-increasing correspondence between the observations and a model-predicted pattern of change, and show that correspondence exists at hemispheric or smaller spatial scales—not only at the surface, but also in the full three-dimensional structure of the atmosphere—then it is less likely that forcing mechanisms other than the ones being considered could match the predicted response pattern. The pattern correlations shown here were computed using annual averages and with pressure- and area-weighted data. Trends in $R(t)$ were relatively insensitive to the choice of averaging period for defining observed anomalies[11].

transition between stratospheric cooling and tropospheric warming[14]. However, the transition height in COMB1 and COMB2 is still roughly 50 hPa higher than in observations (compare Fig. 1*g*, *h* and Fig. 1*j*). There are several possible reasons for this. These include: uncertainties in observed O_3 losses and thus in the simulated temperature changes in the vicinity of the tropopause[15,26]; concerns regarding the validity of the linearity assumption for combining SC-TP and O_3 signals; and the (neglected) effects of upper tropospheric O_3 changes. The coarse vertical resolution of the observed data and most of the model signals also hampers more accurate determination of discrepancies in transition height.

The magnitude of direct anthropogenic sulphate aerosol forcing in TP (roughly $-0.9\,W\,m^{-2}$) is just above the upper end of the range estimated in recent reviews[29,30], although clearly within the range given for total (direct + indirect) sulphate aerosol forcing. It is relevant in this regard that the hemispheric-scale patterns of forcing due to aerosol direct and indirect effects may be similar[31–34]. The effect in COMB3 of halving the temperature response in S-TP relative to C-TP is to reduce the interhemispheric asymmetry in the low- to mid-troposphere and enhance the temperature-change contrast between the stratosphere and troposphere (Fig. 1*i*).

Figure 1*j* shows observed temperature changes, expressed as linear trends over 1963–87. The observations show two prominent features: stratospheric cooling and tropospheric warming, and reduced warming in the Northern Hemisphere between 850 and 300 hPa. These have been documented in previous investigations[3,4,7,35]. The pattern of stratospheric cooling and tropospheric warming is common to the observations and all model signals shown in Fig. 1 (with the exception of the 'ozone-only' and S-TP signals). In the lower atmosphere, it is clear that the observations are in better accord with combined greenhouse-gas and aerosol signals than with 'CO_2-only' signals[10,11].

Model–observed pattern similarity

To compare model and observed vertical temperature-change patterns we use a so-called 'centred' correlation statistic[11], $R(t)$:

$$R(t) = \left[\sum_{x=1}^{n}(\Delta D(x,t) - \widehat{\Delta D}(t))(\Delta M(x) - \widehat{\Delta M})\right] \Big/ [n s_D(t) s_M] \quad (1)$$

ΔD and ΔM are temperature-change fields for observed data and model output, respectively, and x and t are discrete indices over space ($x = 1, \ldots n$, the combined latitude–height dimension of the radiosonde data) and time ($t = 1963, \ldots 1987$). Observed changes are anomalies relative to the average over 1963–73, and model changes are differences between time averages of perturbation and control experiments (see Fig. 1). The $\widehat{\ }$ indicates a spatial average. The observed spatial variance $s_D^2(t)$ is

$$s_D^2(t) = \sum_{x=1}^{n}\left[\Delta D(x,t) - \widehat{\Delta D}(t)\right]^2 \Big/ (n-1) \quad (2)$$

with the model spatial variance s_M^2 defined similarly.

If the observed time-varying patterns of temperature change are becoming increasingly similar to the model-predicted responses, the $R(t)$ statistic will show a sustained positive trend[36]. This trend is unlikely to be linear and monotonic, as the observations reflect a response to the real (as opposed to the modelled) anthropogenic forcing and to other human-induced and natural forcings not included in the model experiments. Additionally, any overall $R(t)$ trend will be modulated by internally

TABLE 1 Significance test results

Season	Signal	Trend lengths (years) 10 MPI	10 GFDL	10 HC	15 MPI	15 GFDL	15 HC	25 MPI	25 GFDL	25 HC
a 50–850 hPa										
DJF	C-TP	0.01	0.00	0.05	0.00	0.00	0.01	0.00	0.00	0.00
	C-HC	0.06	0.03	0.21	0.02	0.00	0.09	0.01	0.00	0.02
	SC-TP	0.02	0.02	0.12	0.00	0.00	0.02	0.00	0.00	0.00
	SC-HC	0.07	0.02	0.23	0.02	0.00	0.11	0.00	0.00	0.01
	COMB1	0.02	0.04	0.05	0.00	0.00	0.00	0.00	0.00	0.00
	COMB2	0.02	0.05	0.03	0.00	0.00	0.00	0.00	0.00	0.00
	COMB3	0.01	0.00	0.05	0.00	0.00	0.01	0.00	0.00	0.00
JJA	C-TP	0.08	0.20	0.25	0.02	0.08	0.16	0.00	0.00	0.00
	C-HC	0.23	0.35	0.39	0.07	0.17	0.22	0.00	0.00	0.00
	SC-TP	0.10	0.17	0.24	0.07	0.10	0.20	0.00	0.00	0.00
	SC-HC	0.13	0.25	0.32	0.02	0.10	0.17	0.00	0.00	0.00
	COMB1	0.10	0.18	0.20	0.06	0.10	0.14	0.00	0.00	0.00
	COMB2	0.10	0.20	0.20	0.05	0.11	0.14	0.00	0.00	0.00
	COMB3	0.10	0.19	0.24	0.05	0.09	0.15	0.00	0.00	0.00
ANN	C-TP	0.16	0.24	0.33	0.01	0.01	0.11	0.00	0.00	0.00
	C-HC	0.20	0.26	0.36	0.04	0.04	0.19	0.00	0.00	0.01
	SC-TP	0.23	0.27	0.38	0.04	0.03	0.15	0.00	0.00	0.00
	SC-HC	0.20	0.26	0.36	0.05	0.04	0.18	0.00	0.00	0.00
	COMB1	0.26	0.34	0.38	0.04	0.04	0.10	0.00	0.00	0.00
	COMB2	0.30	0.38	0.38	0.03	0.05	0.07	0.00	0.00	0.00
	COMB3	0.15	0.21	0.33	0.02	0.01	0.13	0.00	0.00	0.00
b 500–850 hPa										
DJF	C-TP	0.08	0.15	0.20	0.06	0.12	0.15	0.08	0.12	0.25
	C-HC	0.55	0.53	0.53	0.49	0.51	0.48	0.20	0.28	0.27
	SC-TP	0.29	0.37	0.40	0.30	0.38	0.36	0.01	0.04	0.02
	SC-HC	0.48	0.50	0.47	0.51	0.52	0.50	0.00	0.02	0.01
	COMB1	0.20	0.29	0.29	0.32	0.37	0.36	0.00	0.03	0.01
	COMB2	0.16	0.26	0.21	0.33	0.39	0.37	0.00	0.02	0.01
	COMB3	0.10	0.17	0.19	0.12	0.21	0.18	0.07	0.11	0.09
JJA	C-TP	0.34	0.46	0.43	0.45	0.48	0.43	0.55	0.51	0.44
	C-HC	0.81	0.66	0.63	0.50	0.52	0.46	0.53	0.51	0.52
	SC-TP	0.17	0.28	0.31	0.18	0.29	0.28	0.02	0.11	0.10
	SC-HC	0.20	0.31	0.31	0.22	0.33	0.31	0.01	0.04	0.06
	COMB1	0.18	0.28	0.30	0.20	0.29	0.28	0.02	0.11	0.09
	COMB2	0.20	0.28	0.29	0.21	0.31	0.28	0.03	0.12	0.09
	COMB3	0.19	0.33	0.36	0.21	0.33	0.33	0.07	0.16	0.13
ANN	C-TP	0.24	0.37	0.36	0.32	0.43	0.41	0.27	0.40	0.37
	C-HC	0.66	0.57	0.54	0.61	0.55	0.52	0.44	0.47	0.43
	SC-TP	0.29	0.41	0.38	0.22	0.31	0.31	0.00	0.03	0.04
	SC-HC	0.54	0.49	0.48	0.47	0.50	0.49	0.00	0.02	0.02
	COMB1	0.33	0.42	0.40	0.27	0.35	0.34	0.00	0.02	0.03
	COMB2	0.37	0.44	0.41	0.32	0.38	0.37	0.00	0.02	0.00
	COMB3	0.19	0.35	0.34	0.21	0.34	0.33	0.02	0.08	0.06

Significance levels (*p*-values) for seasonal and annual vertical temperature-change signals from the TP and HC experiments with forcing by CO_2 only and CO_2 + aerosols and from the three sensitivity studies (COMB1, COMB2, COMB3). The first column gives the season of interest, while the second column indicates the experiment from which the signal pattern was taken. The remaining columns give the model experiments used to obtain natural variability estimates (on three different timescales). The signals of interest are the linear trends for the most recent 10, 15 and 25 years of the $R(t)$ time series shown in Fig. 2*a* and *b*—that is, the trends over 1978–87, 1973–87, and 1963–87. These trends provide information on the degree of time-increasing pattern similarity between the observations and the model simulations. Distributions of 'unforced' $R(t)$ trends on 10-, 15- and 25-year timescales were generated as described in Fig. 3. Significance levels were then computed by comparing the 'signal' $R(t)$ trends with the appropriate sampling distributions for unforced trends[11]. Shaded boxes denote results that achieve significance at the 5% level or better. In these cases, the time-increasing similarity between model signal patterns and observations is unlikely to be due to (model estimated) internally-generated natural variability. Results are for model–observed comparisons over 50–850 hPa (*a*) and over 500–850 hPa (*b*).

generated natural climate variability. There are two main issues of interest: whether trends in $R(t)$ could be due to natural internal variability alone, and whether they are different for different model signals.

For comparisons over 50–850 hPa (Fig. 2*a*), the behaviour of $R(t)$ is similar for all signals except S-TP: trends are positive over the full 25-year period, indicating an increasing expression of the model-predicted patterns in the observed annually averaged data. These similarities are due partly to the large-amplitude pattern of stratospheric cooling/tropospheric warming common to all signals that incorporate CO_2 effects (see Fig. 1). Differences in the magnitude of this common pattern in the individual signals are reduced since they are scaled by different model spatial variances, s_M^2. Similarities in $R(t)$ are also related to the removal of different spatial mean values (ΔM) from the model signal patterns, which has the effect of making the height of the transition from stratospheric cooling to tropospheric warming more similar in the individual signals.

To focus on hemispheric asymmetry differences in the various signals, we then restricted pattern comparisons to 500–850 hPa (Fig. 2*b*). There is now a clear distinction between CO_2-only signals and signals that additionally incorporate aerosol effects. Annual $R(t)$ time series show overall positive trends for the SC-TP, SC-HC, S-TP, COMB1 and COMB2 signals, but little or no trend for the CO_2-only signals and a smaller positive trend for COMB3. The primary reason for this discrimination is the inter-hemispheric asymmetry common to the observations and the signals with combined CO_2 + aerosol forcing. This common asymmetry occurs also in DJF and JJA.

Although visibly apparent (Fig. 1), the benefit of incorporating stratospheric O_3 effects is not clearly shown in the $R(t)$ results. It becomes more obvious in an uncentred statistic, which retains the spatial means of the two fields being compared. This, however, has other limitations in the context of attributing observed changes to a specific causal factor[11,37].

Trend significance

Are the positive $R(t)$ trends in Fig. 2 unusually large relative to the trends we might expect in the absence of any anthropogenic forcing—that is, due to natural variability of the climate system? To address this issue, we use (internally generated) natural variability information from multi-century CGCM control experiments performed at the Hadley Centre (HC)[10], the Max-Planck Institute for Meteorology in Hamburg (MPI)[38] and GFDL[39]. All integrations were run with no changes in natural external or anthropogenic forcings.

A number of studies have attempted to assess how reliably these three CGCMs simulate real-world natural variability[39–42]. On timescales of 10–30 years there is good agreement between the GFDL and HC spectra and the observed spectrum for global-mean annually averaged near-surface temperature[39,43]. Comparisons of model and observed patterns of surface temperature variability show that similarities exist on timescales of 5–10 years, although there are differences on shorter timescales[39,41,44].

More rigorous validation of the model-estimated internal variability of vertical temperature changes is difficult because the radiosonde record is short and represents a convolution of natural variability and anthropogenic effects. For the purposes of this investigation we must therefore assume that the CGCMs used here provide credible estimates of the spectrum and patterns of internal natural variability on timescales ranging from 10 to 25 years. Our use of noise information from multiple control runs provides an indication of the robustness of our significance estimates to uncertainties in the model-estimated noise.

In the significance-testing procedure[11], each model signal pattern (with the exception of the O_3 and S-TP signals) is correlated with the sequences of vertical temperature-change patterns simulated in each of the three CGCM control runs. The resulting time series provide information on the behaviour of the $R(t)$ statistic in the absence of external forcing. By fitting 10-, 15-, and 25-year linear trends to overlapping chunks of these 'natural' $R(t)$ time series, we generate sampling distributions of unforced $R(t)$ trends. The 'signal' trends in $R(t)$ over the past 10 to 25 years (Fig. 2*a*, *b*) are then compared with these sampling distributions to determine whether changes in model–observed pattern similarity with time are statistically unusual (Fig. 3).

For model–observed comparisons over 500–850 hPa, the positive 25-year $R(t)$ trends for all signals considered (CO_2-only, CO_2 + aerosols, and the three sensitivity studies) differ significantly from unforced trends (Table 1*a*). This result shows that the observed pattern of change over 1963–87 is similar to model-predicted signals that incorporate CO_2 effects, whereas 'natural' patterns of change over 25-year periods are not[45].

On shorter timescales (10 and 15 years) signal-to-noise ratios decrease and significance results show a seasonal dependence, with fewer significant trends for both JJA and annually averaged data. There is also a dependence on the CGCM used to estimate noise properties, with higher noise levels (see Fig. 3) and fewer significant results for noise estimates obtained from the HC control run. The reverse applies for the MPI noise estimates. The 10- and 15-year results show why natural variability makes it difficult to evaluate the significance of short timescale trends, such as the lower tropospheric temperature changes estimated since 1979 from the satellite-based Microwave Sounding Unit[46,47].

Restricting pattern comparisons to 500–850 hPa yields a clear discrimination between the CO_2-only signals and signals that incorporate aerosol effects (Table 1*b*). In DJF and in the annually averaged data, the 25-year $R(t)$ signal trends are highly significant for the SC-TP, SC-HC, COMB1 and COMB2 signals, but not for COMB3 (except for annually averaged data relative to the MPI noise) or the CO_2-only signals. As noted above, this result arises

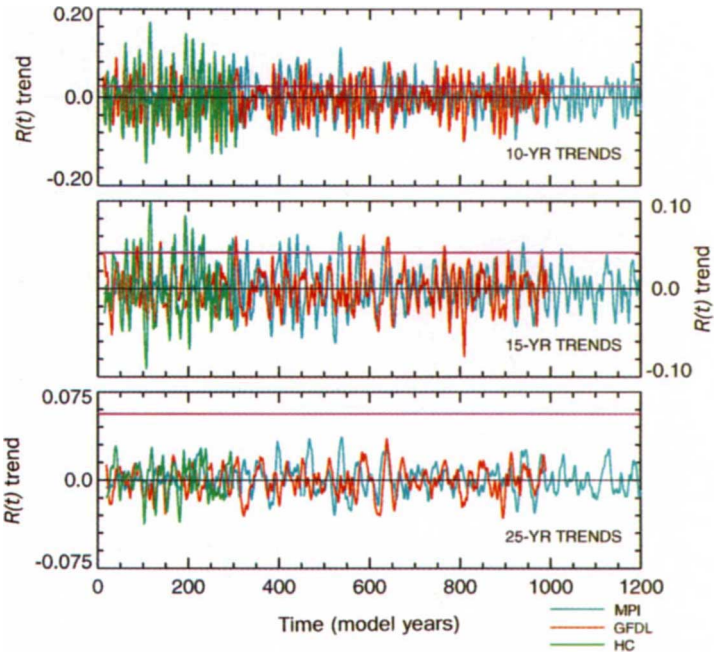

FIG. 3 The relationship between forced and unforced trends in the $R(t)$ pattern similarity statistic. 'Unforced' $R(t)$ time series were computed by correlating the fixed pattern of annually-averaged vertical temperature changes in the SC-TP experiment (Fig. 1*c*) with the time-varying temperature-change patterns form the 310-, 1,000- and 1,260-year HC, GFDL, and MPI control integrations (respectively). Model anomaly patterns were defined relative to the overall time-mean of each control run, and were filtered in the same way as the observations (see Fig. 2). The figure shows the result of fitting overlapping linear trends to 10-, 15- and 25-year segments of the unforced $R(t)$ time series, and then plotting the magnitude (at any point in time) of the linear trend in $R(t)$. The overlap between trends is by all but one year. This yields sampling distributions of all possible unforced $R(t)$ trends for the three selected timescales. The purple horizontal lines in each panel give the magnitude of the $R(t)$ trend for the comparison of the SC-TP signal with observations over 1978–87, 1973–87 and 1963–87 (see Fig. 2*a*). All trends are expressed as the change in $R(t)$ per year. The level of time-increasing similarity between the observed vertical temperature-change patterns and the SC signal over the last 25 years is highly unusual relative to the unforced 25-year $R(t)$ trends estimated from all three control integrations. In contrast, recent 10-year trends in $R(t)$ are not unusual occurrences. Note that the magnitude of the unforced $R(t)$ trends decreases as the length of $R(t)$ trends increases. The results shown here are for annually averaged data and for temperature-change patterns defined over 50–850 hPa. $R(t)$ trends are plotted on the central year of the trend.

mainly from the relatively lower Northern Hemisphere warming that is common to the observations and the combined forcing signals. Again, none of the shorter-timescale trends in $R(t)$ achieve significance at the 5% level or better.

Equilibrium and transient signal similarity

We have shown above that the TP equilibrium and HC transient signals yield very similar detection results when compared with the observed radiosonde data. This does not necessarily signify that the TP and HC signals are *themselves* correlated. Such similarity between equilibrium and transient signal patterns is implicitly assumed in any detection study that makes use of equilibrium signals[48]. To test this assumption in a rigorous way would require signal estimates from both types of experiment performed with the same model. These were not available here. We gain some indication of the similarity between equilibrium and transient results by computing pattern correlations (see equation (1)) between the TP and HC signals over the 50–850 hPa and 500–850 hPa domains. For the full vertical domain, the key correlations for annually averaged data (and for HC signals that are decadal averages for the 1990s) are $R\{\text{C-TP:C-HC}\} = 0.87$; $R\{\text{SC-TP:SC-HC}\} = 0.85$. For the low- to mid-troposphere the key result is $R\{\text{SC-TP:SC-HC}\} = 0.61$. Note, however, that the CO_2-only signals in the TP and HC experiments are uncorrelated over 500–850 hPa ($R\{\text{C-TP:C-HC}\} = -0.05$).

A further assumption underlying our detection strategy is that the transient signal is relatively stable with time over the period relevant for a comparison with observations[48]. We tested this by computing correlations between decadally averaged HC signal patterns for the modelled '1980s' and '1990s' $R\{\text{C-HC80:C-HC90}\} = 0.97$; $R\{\text{SC-HC80:SC-HC90}\} = 0.98$ (for 50–850 hPa) and $R\{\text{SC-HC80:SC-HC90}\} = 0.93$ (for 500–850 hPa).

These results illustrate that the signal components of most interest here—stratospheric cooling/tropospheric warming (in experiments that incorporate CO_2 effects) and hemispheric-scale temperature asymmetry (in experiments that include aerosol effects)—are similar in the TP and HC experiments and are relatively stable over the time period of the HC integrations relevant for comparison with the radiosonde data. We note, however, that these findings are not necessarily of general applicability to different models, climate variables and geographical domains.

Conclusions

Our results suggest that the similarities between observed and model-predicted changes in the zonal-mean vertical patterns of temperature change over 1963–87 are unlikely to have resulted from natural internally generated variability of the climate system. This conclusion holds for pattern comparisons over 50–850 hPa, which focus on the large-amplitude signal of stratospheric cooling and tropospheric warming, and for comparisons over 500–850 hPa, which emphasize hemispheric-scale temperature asymmetries in the lower atmosphere. Stratospheric cooling and tropospheric warming are common to the observations and all signals that incorporate CO_2 effects, whereas hemispheric asymmetry is an observed feature that is found only in model experiments that incorporate aerosol effects.

The main uncertainties in our work relate to:

(1) Estimates of the relative magnitudes and spatial and temporal evolution of the different forcings[29,30], including those human factors represented here (greenhouse gases, direct sulphate aerosol effects and stratospheric ozone), those not specifically represented here (such as indirect aerosol effects[31,32,49], other anthropogenic aerosols[50–52], tropospheric ozone and other non-CO_2 greenhouse gases[53]), and purely natural forcings (for example, variations in solar output and volcanic aerosol loadings).

(2) The simulated response to forcing, including model-dependent factors such as global and regional sensitivity, which in turn depend on model parametrizations (for example, for clouds, which directly affect global sensitivity[54], and for oceanic vertical mixing, which may affect interhemispheric asymmetry).

(3) The realism of CGCM-derived estimates of natural internal variability on decadal and longer timescales[55], and the neglect of the variability arising from natural external forcings.

(4) The existence of time-varying instrumental biases in the radiosonde data, and their incomplete spatial coverage[7,8,56,57].

Where possible, we have attempted to explore the sensitivity of our principal results to these uncertainties. For comparisons focusing on the pattern of stratospheric cooling and tropospheric warming, we have shown that the significant 25-year $R(t)$ trends are seasonally robust. They are insensitive to uncertainties in the signals examined here (as shown by our use of equilibrium and transient signals from models with differences in physical processes and in their treatment of direct aerosol effects), in the magnitude of the direct aerosol forcing (as shown by COMB3), and in the incorporation of stratospheric O_3 effects (as shown by COMB1 and COMB2). Finally, they are robust to uncertainties in the CGCM estimates of natural internal climate variability used here—to achieve non-significant results on 25-year timescales would require noise levels for 'unforced' $R(t)$ trends to be roughly twice as large as those estimated here.

The situation is more equivocal for model–observed comparisons focusing on hemispheric temperature-change asymmetries in the lower atmosphere. Here, too, the 25-year $R(t)$ temperature trends are generally robust to CGCM differences in natural internal variability and to signal uncertainties arising from model differences in physical processes and in the representation of direct aerosol effects. They are, however, sensitive to uncertainties in the magnitude of the aerosol forcing (as shown by COMB3). Although this points towards the need for caution in the interpretation of our results, we note that the observations are in better agreement with the larger aerosol forcing and hemispheric asymmetry in COMB1 and COMB2 than with the reduced forcing and asymmetry in COMB3. This may reflect our effective incorporation of some of the pattern characteristics of indirect aerosol forcing in the response to direct forcing[27]. For this to be the case would require a hemispherically asymmetric indirect aerosol effect, and there is evidence to support this in recent modelling studies[31,32] and satellite observations of interhemispheric differences in cloud liquid-water droplet size[33].

This investigation shows the clear need for modelling experiments with simultaneous changes in CO_2, O_3 and anthropogenic sulphate aerosols. Our use of linear superposition to assess the possible effects of ozone changes on a CO_2 + aerosol signal should be regarded as a sensitivity study only. The incorporation of stratospheric O_3 effects in this way improves the fit with observations by reducing the height of the transition from stratospheric cooling to tropospheric warming. The implication of this result and other recent work[14,15] is that climate-change detection investigations that ignore possible ozone effects are likely to be searching for a sub-optimal signal (at least in terms of vertical temperature changes).

There is scope to reduce uncertainties in the observational data. We tested the robustness of our results to these uncertainties by comparing the radiosonde data with a reanalysis of operationally produced climate data. At present, this comparison is only possible after 1979. The extension of this reanalysis back to the early 1960s will allow better evaluation of the reliability of long-term trends in the radiosonde data. This will also be facilitated by other reanalysis efforts[58] and compilations of quality-controlled radiosonde data[57,59].

Although we have identified a component of the observational record that shows a statistically significant similarity with model predictions, we have not quantified the relative magnitude of natural and human-induced climate effects. This will require improved histories of radiative forcing due to natural and anthropogenic factors, and numerical experiments that better define an anthropogenic climate-change signal and the variability due to purely natural causes. □

Received 9 April; accepted 30 May 1996.

1. Madden, R. A. & Ramanathan, V. *Science* **209,** 763–768 (1980).
2. Epstein, E. S. *J. appl. Met.* **21,** 1172–1182 (1982).
3. Karoly, D. J. *Geophys. Res. Lett.* **14,** 1139–1141 (1987).
4. Karoly, D. J. *Geophys. Res. Lett.* **16,** 465–468 (1989).
5. Schlesinger, M. E. & Mitchell, J. F. B. *Rev. Geophys.* **25,** 760–798 (1987).
6. Mitchell, J. F. B., Manabe, S., Meleshko, V. & Tokioka, T. in *Climate Change: The IPCC Scientific Assessment* (eds Houghton, J. T., Jenkins, G. J. & Ephraums, J. J.) 131–172 (Cambridge Univ. Press, 1990).
7. Karoly, D. J. *et al. Clim. Dyn.* **10,** 97–105 (1994).
8. Oort, A. H. & Liu, H. *J. Clim.* **6,** 292–307 (1993).
9. Taylor, K. E. & Penner, J. E. *Nature* **369,** 734–737 (1994).
10. Mitchell, J. F. B., Johns, T. C., Gregory, J. M. & Tett, S. F. B. *Nature* **376,** 501–504 (1995).
11. Santer, B. D. *et al. Clim. Dyn.* **12,** 77–100 (1995).
12. Prather, M. *et al.* in *Climate Change 1994: Radiative Forcing of Climate Change and an Evaluation of the IPCC IS92 Emission Scenarios* (eds Houghton, J. T. *et al.*) 73–126 (Cambridge Univ. Press, 1994).
13. Hansen, J. E., Lacis, A., Ruedy, R., Sato, M. & Wilson, H. *Nat. geogr. Res. Expl.* **9,** 142–158 (1993).
14. Hansen, J. E. *et al. Clim. Change* **30,** 103–117 (1995).
15. Ramaswamy, V., Schwarzkopf, M. D. & Randel, W. J. *Nature* (submitted).
16. Walton, J. J., MacCracken, M. C. & Ghan, S. J. *J. geophys. Res.* **93,** 8339–8354 (1988).
17. Penner, J. E., Atherton, C. A. & Graedel, T. E. in *Global Atmospheric-Biospheric Chemistry* (ed. Prinn, R.) 223–248 (Plenum, New York, 1994).
18. Taylor, K. E. & Ghan, S. J. *J. Clim.* **5,** 906–919 (1992).
19. Charlson, R. J. & Wigley, T. M. L. *Scient. Am.* **270,** 48–57 (1994).
20. Johns, T. C. *et al. Clim. Dyn.* (submitted).
21. Houghton, J. T., Callander, B. A. & Varney, S. K. (eds) *Climate Change 1992: The Supplementary Report to the IPCC Scientific Assessment* (Cambridge Univ. Press, 1992).
22. Mitchell, J. F. B., Davis, R. A., Ingram, W. J. & Senior, C. A. *J. Clim.* **8,** 2364–2386 (1995).
23. Karl, T. R. *Nature* **371,** 380–381 (1994).
24. Christy, J. R. *Clim. Change* **31,** 455–474 (1995).
25. Kalnay, E. *et al. Bull. Am. met. Soc.* **77,** 437–471 (1996).
26. Mahlman, J. D., Pinto, J. P. & Umscheid, L. J. *J. atmos. Sci.* **51,** 489–508 (1994).
27. Penner, J. E., Wigley, T. M. L., Jaumann, P., Santer, B. D. & Taylor, K. E. in *Communicating About Climate: the Story of the Model Evaluation Consortium for Climate Assessment* (eds Howe, W. & Henderson-Sellers, A.) (Gordon & Breach, in the press).
28. Ramaswamy, V. & Bowen, M. M. *J. geophys. Res.* **99,** 18909–18921 (1994).
29. Shine, K. P., Fouquart, Y., Ramaswamy, V., Solomon, S. & Srinivasan, J. in *Climate Change 1994: Radiative Forcing of Climate Change and an Evaluation of the IPCC IS92 Emission Scenarios* (eds Houghton, J. T. *et al.*) 163–203 (Cambridge Univ. Press, 1994).
30. Shine, K. P., Fouquart, Y., Ramaswamy, V., Solomon, S. & Srinivasan, J. in *Climate Change 1995: The Science of Climate Change* (eds Houghton, J. T. *et al.*) 108–118 (Cambridge Univ. Press, 1996).
31. Jones, A., Roberts, D. L. & Slingo, A. *Nature* **370,** 450–453 (1994).
32. Erickson, D. J., Oglesby, R. J. & Marshall, S. *Geophys. Res. Lett.* **22,** 2017–2020 (1995).
33. Boucher, O. *J. Clim.* **8,** 1403–1409 (1995).
34. Chuang, C. C., Penner, J. E., Taylor, K. E., Grossmann, A. S. & Walton, J. J. *J. geophys. Res.* (submitted).
35. Angell, J. K. *J. Clim.* **1,** 1296–1313 (1988).
36. Barnett, T. P. & Schlesinger, M. E. *J. geophys. Res.* **92,** 14772–14780 (1987).
37. Wigley, T. M. L. & Barnett, T. P. in *Climate Change: The IPCC Scientific Assessment* (eds Houghton, J. T., Jenkins, G. J. & Ephraums, J. J.) 239–255 (Cambridge Univ. Press, 1990).
38. Hasselmann, K. *et al. Rep. No. 168* (Max-Planck-Institut für Meteorologie, Hamburg, 1995).
39. Stouffer, R. J., Manabe, S. & Vinnikov, K. Ya. *Nature* **367,** 634–636 (1994).
40. Tett, S., Johns, T. C. & Mitchell, J. F. B. *Clim. Dyn.* (submitted).
41. Manabe, S. & Stouffer, R. J. *J. Clim.* **9,** 376–393 (1996).
42. Hegerl, G. C. *et al. J. Clim.* (in press).
43. Santer, B. D., Wigley, T. M. L., Barnett, T. P. & Anyamba, E. in *Climate Change 1995: The Science of Climate Change* (eds Houghton, J. T. *et al.*) 407–443 (Cambridge Univ. Press, 1996).
44. Gates, W. L. *et al.* in *Climate Change 1995: The Science of Climage Change* (eds Houghton, J. T. *et al.*) 229–284 (Cambridge Univ. Press, 1996).
45. Vinnikov, K. Ya., Robock, A., Stouffer, R. J. & Manabe, S. *Geophys. Res. Lett.* (in the press).
46. Christy, J. R. & McNider, R. T. *Nature* **367,** 325 (1994).
47. Jones, P. D. *Geophys. Res. Lett.* **21,** 1149–1152 (1994).
48. Barnett, T. P., Schlesinger, M. E. & Jiang, X.-J. in *Greenhouse-Gas-Induced Climatic Change: A Critical Appraisal of Simulations and Observations* (ed. Schlesinger, M. E.) 537–558 (Elsevier, Amsterdam, 1991).
49. Wigley, T. M. L. *Nature* **339,** 365–367 (1989).
50. Penner, J. E., Dickinson, R. & O'Neill, C. *Science* **256,** 1432–1434 (1992).
51. Tegen, I. & Fung, I. *J. geophys. Res.* **100,** 18707–18726 (1995).
52. Penner, J. E. *et al. Bull. Am. met. Soc.* **75,** 375–400 (1994).
53. Wang, W.-C., Dudek, M. P., Liang, X.-Z. & Kiehl, J. T. *Nature* **350,** 573–577 (1991).
54. Mitchell, J. F. B., Senior, C. A. & Ingram, W. J. *Nature* **341,** 132–134 (1989).
55. Barnett, T. P., Santer, B. D., Jones, P. D., Bradley, R. S. & Briffa, K. R. *Holocene* (in the press).
56. Gaffen, D. J. *J. geophys. Res.* **99,** 3667–3676 (1994).
57. Parker, D. E. & Cox, D. I. *Int. J. Climatol.* **15,** 473–496 (1995).
58. Trenberth, K. E. *Clim. Change* **31,** 427–453 (1995).
59. Eskridge, R. E. *et al. Bull. Am. met. Soc.* **76,** 1759–1775 (1995).

ACKNOWLEDGEMENTS. We thank J. Boyle, M. Fiorino, D. Gaffen, L. Gates, T. Karl, J. Mahlman, S. Manabe, A. Robock, H. Rodhe and four reviewers for helpful suggestions; L. Corsetti (PCMDI) for providing programming assistance; J.-S. von Storch and G. Hegerl for supplying data from the MPI control integration; and D. Williams, R. Mobley and R. Drach for developing software used to produce the colour graphics. Work at Lawrence Livermore National Laboratory was performed under the auspices of the US Department of Energy, Environmental Sciences Division. Support for T.J., J.M. and S.T. was provided by the UK Department of the Environment. T.M.L.W. and P.D.J. were supported by the US Department of Energy, Environmental Sciences Division. T.M.L.W. was also supported under the NOAA Climate Change, Data and Detection Program. The MECCA Program supplied some of the computer time required for the TP integrations.

CORRESPONDENCE should be addressed to B.D.S. (e-mail: bsanter@rainbow.llnl.gov).